J Soils Sediments (2016) 16:438–448
DOI 10.1007/s11368-015-1252-x

SOILS, SEC 2 • GLOBAL CHANGE, ENVIRON RISK ASSESS, SUSTAINABLE LAND USE • RESEARCH ARTICLE

Comparison of field portable XRF and aqua regia/ICPAES soil analysis and evaluation of soil moisture influence on FPXRF results

Arnaud Robin Schneider[1] · **Benjamin Cancès**[1] · **Clément Breton**[1] · **Marie Ponthieu**[1] · **Xavier Morvan**[1] · **Alexandra Conreux**[1] · **Béatrice Marin**[1]

Received: 9 March 2015 / Accepted: 27 August 2015 / Published online: 9 September 2015
© Springer-Verlag Berlin Heidelberg 2015

Abstract
Purpose Field portable X-ray fluorescence (FPXRF) technology can offer a rapid and cost-effective determination of the total elemental concentrations in soils. The aims of this study were (i) to test the capability of FPXRF to predict the element concentrations of a very large soil sample set and (ii) to assess the influence of soil moisture, known to strongly affect the quality of FPXRF analyses.
Materials and methods A large set of 215 soil samples were analysed for Ba, Ca, Cr, Cu, Fe, Mn, Pb, Rb, Sn, Sr and Zn by inductively coupled plasma atomic emission spectroscopy (ICPAES) after aqua regia digestion and with a FPXRF analyser using a short acquisition time. Soil samples were then saturated with ultrapure water to test the influence of soil water content on FPXRF signal.
Results and discussion For all of the elements, the total concentrations obtained with ICPAES and FPXRF showed a very high degree of linearity, indicating that FPXRF can effectively predict element concentrations in soils. A Lambert-Beer law was successfully used to describe the decrease in the FPXRF concentrations with increasing soil moisture. The attenuation coefficient obtained for each element allowed us to satisfactorily predict the FPXRF concentrations of samples for water contents as high as 136.8 %.
Conclusions These results show that the effect of water on signal attenuation can be corrected and that FPXRF may gradually replace chemical methods for the analysis of environmental samples.

Keywords FPXRF · Soil · Trace elements · Water content

Responsible editor: Fanghua Hao

✉ Arnaud Robin Schneider
arnaud.schneider@univ-reims.fr

[1] Groupe d'Etude sur les Géomatériaux et les Environnements Naturels, Anthropiques et Archéologiques (GEGENAA, EA 3795), Université de Reims Champagne-Ardenne, 2 esplanade Roland Garros, 51100 Reims, France

1 Introduction

In recent years, due to the development of field portable X-ray fluorescence (FPXRF), numerous studies have used X-ray fluorescence to determine element concentrations in environmental samples. This technique has been used in many scientific fields, such as soil science, archaeology and mining (Potts et al. 1995; Papadopoulou et al. 2004; Scheid et al. 2009; Frahm 2013; Gauss et al. 2013; Speakman and Steven Shackley 2013). This method features many advantages compared to chemical analyses. It is non-destructive and cost-effective (compared to conventional laboratory methods) and offers an extremely rapid on-site determination of total elemental concentrations. With the new generation of FPXRF and more sensitive X-ray detectors, less than 2 min is necessary to simultaneously analyse a wide range of elements (Radu and Diamond 2009; Weindorf et al. 2014). This technique is of peculiar use for the rapid mapping and delimiting of contaminated areas or ore areas (Argyraki et al. 1997; Hürkamp et al. 2009; Arenas et al. 2011; Higueras et al. 2012). Although numerous previous studies have reported that results obtained by FPXRF were strongly correlated with those obtained by chemical methods (Bernick et al. 1995a, b; Ramsey et al. 1995; Somogyi et al. 1997; Kilbride et al. 2006; Laperche and Billaud 2008; Radu and Diamond 2009), none has dealt with a sample set exceeding 100 samples.

Several parameters are known to affect the quality and the precision of FPXRF analyses: sample matrix, interfering elements, sample homogeneity, particle size (Clark et al. 1999; Kalnicky and Singhvi 2001; Laperche 2005; Binstock et al. 2008) and soil moisture (Ge et al. 2005; Kido et al. 2006; Tjallingii et al. 2007; Parsons et al. 2013; Weindorf et al. 2014). The latter parameter is one of the most important sources of error, especially when the soil moisture is higher than 20 % (Laiho and Perämäki 2005). Soil water absorbs the primary X-ray radiation from the source and the characteristic X-rays of the analytes. This phenomenon results in an exponential decrease in characteristic X-rays (Ge et al. 2005). Water also causes the primary radiation to scatter, increasing the intensity of scattered X-rays in the fluorescence spectrum. The magnitude of the soil moisture effect, however, depends on the studied elements. Indeed, certain authors have shown that heavier elements are less influenced by soil moisture, in terms of an exponential decrease in the signal (Ge et al. 1997, 2005).

In this context, the objectives of this study were as follows:

1. To test the capability of FPXRF to predict the element concentrations of a very large soil sample set (215 samples) covering a wide range of concentrations and physicochemical properties. The concentrations of Ba, Ca, Cr, Cu, Fe, Mn, Pb, Rb, Sn, Sr and Zn obtained by FPXRF were compared to those determined by emission spectroscopy (inductively coupled plasma atomic emission spectroscopy (ICPAES)) following aqua regia digestion. This chemical method was chosen because it is widely used to determine the trace element concentrations in soils samples.
2. To evaluate the influence of soil moisture on FPXRF readings for each studied element and to establish moisture correction equations to predict the actual concentrations in dry soil samples.

2 Materials and methods

2.1 Soil samples and element concentrations

A total of 215 soil samples were collected from 13 sites in temperate (Champagne-Ardenne, north-eastern of France) and semi-arid areas (western Niger, Sahelian zone). The samples mainly corresponded to the topsoil horizons of the soil profiles. Among these soils, 57 were agricultural soils, 59 were vineyard soils, and 99 were affected by direct or diffuse industrial pollution. The 215 soil samples possessed a wide range of physicochemical characteristics (Table 1).

The soil samples were air-dried or dried in a conventional oven at 40 °C until a constant weight was achieved. The samples were then sieved using a 2-mm-mesh stainless steel sieve and ground to a fine powder (<100 μm) with an agate mortar and pestle. The major and trace element concentrations were determined by ICPAES analyses following aqua regia digestion. Eleven major and trace elements were studied: Ba, Ca, Cr, Cu, Fe, Mn, Pb, Rb, Sn, Sr and Zn. The broad concentration ranges are presented in Table 1.

Table 1 Element concentrations (mg kg^{-1}) in soil samples obtained by aqua regia extraction/ICPAES analysis ($85<n<215$) and $CaCO_3$ and organic carbon contents (wt%)

	n[a]	Mean	Min	Max	First quartile	Median	Third quartile
Ba	127	365.3	10.3	2112.5	41.4	177.7	470.8
Ca	127	142,927	102.4	330,000	89,450	169,300	201,667
Cr	215	70.9	1.9	1817	27.4	46.9	70.4
Cu	214	302.9	0.5	8869	20.1	91.4	217.4
Fe	215	16,215	1361	150,800	4867	7380	20,650
Mn	215	276.4	1.9	1528	119.0	159.0	363.1
Pb	215	347.0	1.3	9048	13.5	64.9	210.0
Rb	99	8.7	2.9	14.1	6.6	8.9	10.6
Sn	85	28.7	0.4	97.3	7.5	26.8	40.3
Sr	127	371.3	4.9	841.9	320.8	431.8	492.9
Zn	215	766.9	1.3	8839	62.1	215.3	699.3
$CaCO_3$	215	34.3	0.0	92.8	12.0	34.4	54.4
OC	215	4.0	0.1	23.7	1.6	3.2	5.3

[a] n is comprised between 85 and 215 because some element concentrations were below the detection limits for some samples

2.2 FPXRF analyses

The basic principle of the X-ray fluorescence method is based on the excitement of the atoms in a sample by an X-ray beam. The inner shell electrons are ejected, causing electrons from higher shells to fill the vacancy. Each of these electron transitions yields fluorescent X-ray photons that are characteristic of that element. The analysis of the excited spectrum allows the quantification of the sample's elemental composition.

A portable Thermo Scientific Niton XL3t 980 Geometrically Optimised Large area Drift Detector (GOLDD+) energy-dispersive XRF (EDXRF) analyser was used. The analyser was equipped with a silver anode operating at a maximum of 50 kV and 40 μA. All analyses were performed with a portable test stand in the laboratory. The elemental concentrations were calculated via the built-in algorithm and a factory calibration (Soil Mode).

A 31-mm X-ray sample cup was filled with approximately 6 g of powdered soil and covered with 6-μm X-ray Mylar® film. The soil powder was compacted with an agate pestle to press the sample against the window film.

2.3 Reference materials and measurement time

The average deviation of the FPXRF technique was verified with four certified reference materials: San Joaquin (SRM 2709a) supplied by National Institute of Standards and Technology (NIST, USA; (Mackey et al. 2010)) and RM Till-4, USGS SAR-M and RCRA 1 supplied by Niton (Table 2). These materials are used worldwide for quality assurance by various laboratories involved in the determination of major, minor and trace element concentrations in soils. In this study, the concentrations were determined at five different times: 60, 90, 120, 180 and 240 s.

The average deviation is calculated for each element as follows:

$$\text{Average deviation}_{\text{Elt}} = \frac{1}{n}\sum_{i=1}^{n}\left[\frac{\left|C_{Ri}^{\text{Elt}} - C_{\text{FPXRF}}^{\text{Elt}}\right|}{C_{Ri}^{\text{Elt}}}\right] \times 100 \quad (1)$$

where n is the number of reference material values, C_{Ri}^{Elt} is the certified concentration of the element in the reference material Ri (Table 2), and $C_{\text{FPXRF}}^{\text{Elt}}$ is the concentration of the element determined using FPXRF.

2.4 Water content

To assess the influence of soil moisture on FPXRF signal absorption, the 215 dried and ground soil samples were analysed by FPXRF and then saturated with ultrapure water (18.2 mΩ cm) in the sample cups. The soil samples were exposed to ambient air for 2 days to reduce their moisture. The samples were then analysed by FPXRF after wetting and after 2 days of air exposure.

The water content was calculated with the following equation:

$$\text{water content}(\%) = \frac{(\omega_w - \omega_d)}{\omega_d} \times 100 \quad (2)$$

where ω_w and ω_d are the weights of the wet sample (after saturation or 2 days of air exposure) and the dried sample, respectively.

The obtained gravimetric water contents ranged from 18 to 136 % after saturation and from 0 to 109 % after 2 days of air exposure.

2.5 Statistical analyses

Statistical analyses were performed using Origin 9.0.0 and Xlstat 7.5.2.

2.5.1 Linear regression

For each element, a linear regression model was used to investigate the relationship between the concentrations obtained by aqua regia/ICPAES and those measured by FPXRF. The relationship produced a linear model:

$$y = ax + b + \varepsilon \quad (3)$$

where y is the FPXRF concentration, x is the aqua regia/ICPAES concentration, b is the intercept of the regression line, a is the slope, and ε is the residual.

The determination coefficient (R^2) was employed as a quality assessment of the fit between the aqua regia/ICPAES and FPXRF data. The p value was used to test the reliability of R^2. This value represents the probability of obtaining a relationship between the two variables assuming that they were not related.

To further assess whether the linear regression was a good predictor of the aqua regia/ICPAES data from the FPXRF results, the mean average percentage error (MAPE) was used:

$$\text{MAPE} = 100 \times \sum_{i=1}^{n}\left|\frac{y_i - \hat{y}_i}{y_i}\right| \quad (4)$$

This factor estimates the average percentage error given by the difference between the actual values and the fitted values predicted by the model. Because the least squares regression usually gives a larger weight to the high values, the MAPEs of the four quartiles were calculated for each element to assess the influence of low concentrations on the MAPE.

2.5.2 Lambert-Beer law

The X-ray intensities emitted from the elements in the wet samples decrease with increasing water content due to the X-ray absorption effect of the interstitial water. According to

Table 2 Certified concentrations of the reference materials (mg kg^{-1})

	Ba	Ca	Cr	Cu	Fe	Mn	Pb	Rb	Sr	Sn	Zn
RM Till-4	395	na	na	237	39,700	490	50	161	109	na	70
SRM 2709a	979	19,100	130	33.9	33,600	529	17.3	99	239	na	103
USGS SAR-M	801	6100	79.7	331	29,900	5220	982	146	151	2.8	930
RCRA 1	1000	na	500	na	na	na	500	na	na	na	na

na not available

Ge et al. (2005), the decrease in the FPXRF results as a function of water content should follow the Lambert-Beer law:

$$\frac{C_{wet}}{C_{dry}} = e^{-\sigma\omega} \quad (5)$$

where C_{wet} is the FPXRF elemental concentration with a water content ω, C_{dry} is the FPXRF elemental concentration in the dry sample, and σ is the attenuation coefficient due to soil moisture.

3 Results and discussion

3.1 Effect of measurement time

Four reference materials were analysed with five different measurement times (60, 90, 120, 180 and 240 s). The average deviations for the 11 elements in the four reference materials are presented as a function of measurement time in Fig. 1. The average deviation was lower than 20 % for Cr, Ba, Mn and Ca and lower than 10 % for Rb, Fe, Pb, Cu and Sr. Zinc is the only element for which the average deviation obviously decreased from 33.6 % for 60 s to 25.1 % for 120 s and then increased to 30.6 % for 240 s. Chromium followed an opposite trend. However, for all elements, the average deviations for measurement times between 60 and 240 s were similar. A Friedman test was used to compare the concentrations of the 11 elements obtained with the five measurement times. There were no significant differences between the five measurement times at the 5 % significance level. These results are not consistent with those of Kilbride et al. (2006) or Laperche and Billaud (2008), who reported better accuracies with increasing measurement time. The larger silicon drift detector of the analyser used in this study might explain the non-significant differences between the five results. The results indicated that a count time of 60 s was appropriate for all analyses and was thus selected for this study. This length of time is similar or close to those used in certain recent works, e.g., 45 s in Radu and Diamond (2009) and 60 s in Weindorf et al. (2014).

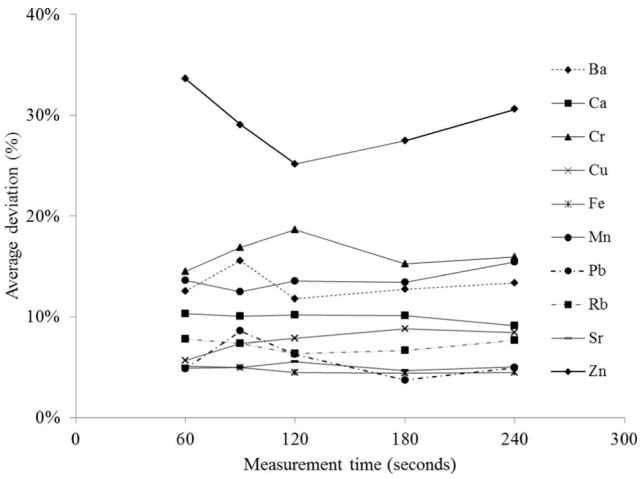

Fig. 1 Average deviation of FPXRF as a function of measurement time

3.2 FPXRF vs. aqua regia/ICPAES concentrations

The results of the linear regressions between aqua regia/ICPAES and FPXRF data are presented in Table 3 and Fig. 2.

Very satisfying correlations (R^2>0.78) were observed between the FPXRF results and aqua regia/ICPAES concentrations for Ba, Ca, Cr, Cu, Fe, Mn, Pb, Sr and Zn.

Because linear regressions are influenced by high values, the prediction of low concentrations by the linear regression can be affected. For all studied elements, the MAPE of the first quartile was systematically the highest. This effect was particularly obvious for Ca and Sr because the distributions of their concentrations were not uniform (Fig. 2b, k). Indeed, only a few soils were non-carbonated in our sample set. Consequently, the MAPE of the first quartile was very high (430.3 % for Ca and 96.1 % for Sr; Table 3). In other words, low Ca and Sr concentrations are poorly estimated by these linear regressions. Contrary to the results for low concentrations, the R^2 and MAPE values of the second, third and fourth quartiles were 0.97 and <11 %, respectively, for Ca and 0.96 and <9 %, respectively, for Sr.

The concentrations of Cr and Mn were underestimated by the FPXRF compared to those determined by aqua regia/ICPAES, especially when the concentrations were high. The same trend was observed for Mn in Kilbride et al. (2006) with a dual isotope source.

The fitted linear model for the Ba data showed that the FPXRF overestimated Ba results at low concentrations (<600 mg kg^{-1}) and underestimated Ba results at high concentrations. However, the comparison of the aqua regia/ICPAES concentrations and the FPXRF results was acceptable even if the intercept (−250.1) increased the MAPE of the first quartile.

For Rb and Sn, the determination coefficients were less satisfactory (R^2=0.4695 and 0.6715, respectively). These results are explained by the low concentrations of these elements in our dataset. The differences between the aqua regia/ICPAES concentrations and the predictions by the linear regression were nevertheless acceptable for Rb and Sn (MAPE <20.1 %).

For Fe, two graphs are presented in Fig. 2. Figure 2e, which includes all data, clearly shows a break in slope for Fe concentrations higher than 10 %. When the data higher than 10 % were removed (Fig. 2f), the value of the slope decreased from 1.56 to 0.97, and the MAPE improved significantly from 72.3 to 18.7 %. The same trend was observed for Zn concentrations higher than 5000 mg kg^{-1} (Fig. 2l). When only the data less than 5000 mg kg^{-1} were taken into account (Fig. 2m), the

Table 3 Statistical parameters of the aqua regia/ICPAES and FPXRF data regressions for Ba, Ca, Cr, Cu, Fe, Fe (<10 %), Mn, Pb, Rb, Sn, Sr, Zn and Zn (<5000 mg kg^{-1})

	n	Aqua regia/ICPAES concentration range (mg kg^{-1})	FPXRF concentration range (mg kg^{-1})	FPXRF mean	FPXRF standard deviation	R^2	*p* value	Significativity of R^2	Slope	Intercept	MAPE (%)	MAPE first quartile (%)	MAPE second quartile (%)	MAPE third quartile (%)	MAPE fourth quartile (%)
Ba	106	10.3–1471.1	71.6–1352.2	456.9	264.4	0.7897	<0.0001	***	0.6126	250.1	34.8	92.2	14.6	15.2	15.9
Ca	127	102.4–330,000.0	1397.0–551,887.9	249,058.2	148,238.7	0.9726	<0.0001	***	1.6750	9656.2	113.8	430.3	10.5	6.5	4.5
Cr	153	4.5–701.4	17.7–472.6	69.6	61.6	0.8190	<0.0001	***	0.6592	17.3	33.7	64.6	25.4	22.0	23.2
Cu	169	2.3–8868.9	22.1–11,664.0	414.7	1358.7	0.9829	<0.0001	***	1.1851	−35.7	45.7	120.0	30.0	14.8	16.2
Fe	215	1360.9–150,800.0	1206.6–265,291.7	17,980.8	36,841.8	0.9366	<0.0001	***	1.5599	−7313.5	72.3	133.7	82.6	29.4	42.8
Fe <10 %	210	1360.9–84,400.0	1206.6–95,256.7	12,648.0	12,471.0	0.9436	<0.0001	***	0.9698	−204.9	18.7	20.4	26.2	15.6	12.9
Mn	181	63.0–1097.4	72.0–846.4	263.8	158.0	0.8937	<0.0001	***	0.6932	67.1	19.5	39.1	12.6	15.0	10.9
Pb	208	1.3–9047.8	5.5–9181.5	381.6	1256.1	0.9853	<0.0001	***	1.0633	0.3	22.9	40.3	20.5	17.2	13.7
Rb	99	2.9–14.1	8.5–44.6	27.0	7.2	0.4695	<0.0001	***	1.9190	10.3	18.2	34.3	11.7	11.9	14.8
Sn	68	0.4–97.3	19.5–115.9	51.3	22.2	0.6715	<0.0001	***	0.8244	22.6	20.1	28.2	16.4	16.5	19.1
Sr	127	4.9–841.9	6.7–835.0	380.8	205.5	0.9590	<0.0001	***	0.9600	24.4	30.0	96.1	7.3	9.0	6.8
Zn	182	10.7–8838.5	14.3–14,888.3	1064.1	2223.5	0.9567	<0.0001	***	1.3980	−198.9	127.3	407.9	58.6	18.6	21.9
Zn <5000 mg kg^{-1}	177	10.7–4602.1	14.3–5102.5	733.0	1019.8	0.9910	<0.0001	***	1.0704	−10.8	17.4	25.8	20.8	16.5	6.3

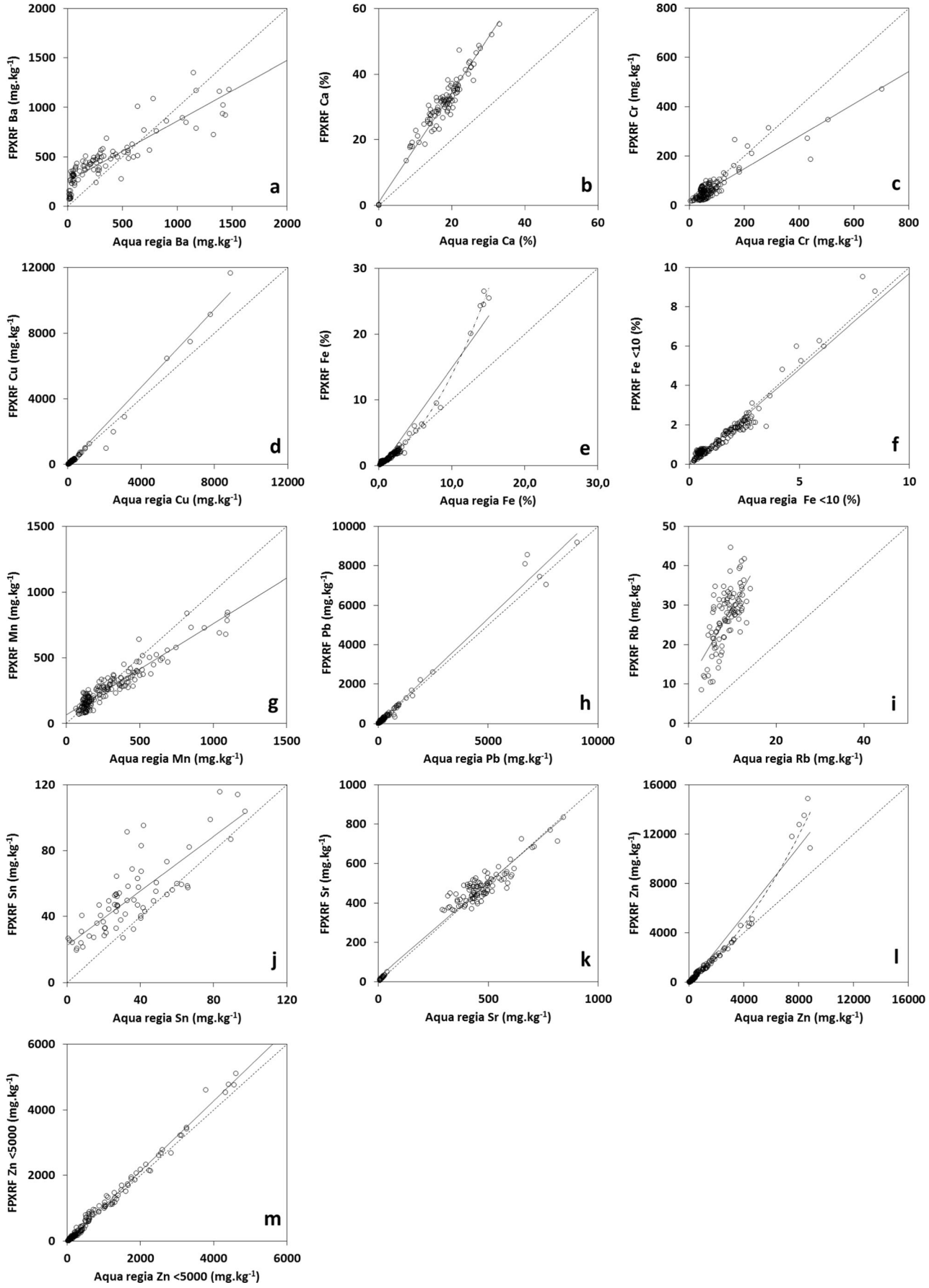
FPXRF Ba (mg.kg-1)
Aqua regia Ba (mg.kg-1)
a
FPXRF Ca (%)
Aqua regia Ca (%)
b
FPXRF Cr (mg.kg-1)
Aqua regia Cr (mg.kg-1)
c
FPXRF Cu (mg.kg-1)
Aqua regia Cu (mg.kg-1)
d
FPXRF Fe (%)
Aqua regia Fe (%)
e
FPXRF Fe <10 (%)
Aqua regia Fe <10 (%)
f
FPXRF Mn (mg.kg-1)
Aqua regia Mn (mg.kg-1)
g
FPXRF Pb (mg.kg-1)
Aqua regia Pb (mg.kg-1)
h
FPXRF Rb (mg.kg-1)
Aqua regia Rb (mg.kg-1)
i
FPXRF Sn (mg.kg-1)
Aqua regia Sn (mg.kg-1)
j
FPXRF Sr (mg.kg-1)
Aqua regia Sr (mg.kg-1)
k
FPXRF Zn (mg.kg-1)
Aqua regia Zn (mg.kg-1)
l
FPXRF Zn <5000 (mg.kg-1)
Aqua regia Zn <5000 (mg.kg-1)
m

◀ **Fig. 2** Regression of FPXRF data versus aqua regia/ICPAES concentrations of **a** Ba, **b** Ca, **c** Cr, **d** Cu, **e** Fe, **f** Fe lower than 10 %, **g** Mn, **h** Pb, **i** Rb, **j** Sn, **k** Sr, **l** Zn and **m** Zn lower than 5000 mg kg^{-1}. The regression lines (*straight lines*), the regression curves for Fe and Zn (*curved lines*) and the relation $y=x$ (*dashed lines*) are shown

slope, MAPE and R^2 values were better than those of the entire dataset (1.07 vs. 1.40, 17.4 vs. 127.3 % and 0.9910 vs. 0.9567, respectively). These results for Fe and Zn are consistent with Laperche (2005), even though the breaks in slope

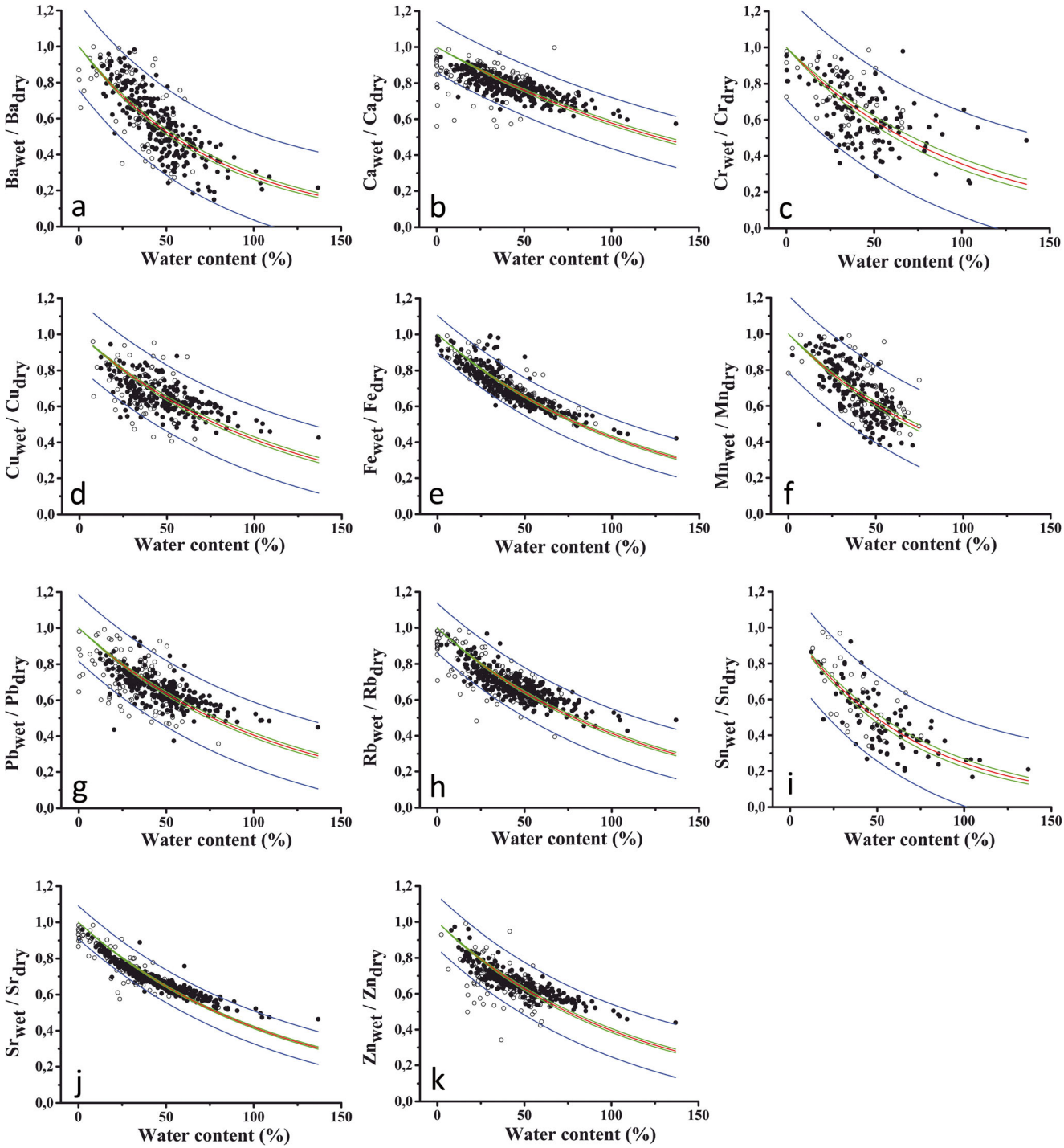

Fig. 3 Relationship between the attenuation of measured FPXRF concentrations (concentration of element *i* for wet samples normalised by the concentration for dry samples) and the water content. The *solid lines* (in *red*) for each element are the regression curves calculated using Eq. (5) with confidence (in *green*) and prediction (in *blue*) bands (95 %). The *open circles* correspond to the first quartile of the dataset

were observed at different concentrations (6 % for Fe and 1 % for Zn). These differences are likely due to different factory calibrations between the used analysers. The breaks in slope could be corrected by manually calibrating the analyser instead of using the factory calibration, but this was not the purpose of this study. These results mean that the Soil Mode of the FPXRF analyser used in this study is not suitable to precisely quantify very high Fe and Zn concentrations in soils.

For Fe (<10 %), Pb, Sr and Zn (<5000 mg kg^{-1}), the regression lines were close to $y=x$. This outcome demonstrates that the FPXRF results are similar to the aqua regia/ICPAES concentrations and that the FPXRF analyser is a useful and satisfactory tool for determining element concentrations in soils. These results are consistent with those of Kilbride et al. (2006).

3.3 Influence of soil moisture on FPXRF

The influence of water content on the FPXRF measurements is presented in Fig. 3. The FPXRF concentrations exponentially decrease with increasing water content as demonstrated in previous studies (Ge et al. 2005; Tjallingii et al. 2007). The attenuation of FPXRF concentrations due to water content was fitted using the Lambert-Beer equation (Eq. 5, Table 4).

Many studies have already tested the effect of water on X-ray fluorescence, but none has used as large a dataset as in the present study (Ge et al. 2005; Kido et al. 2006; Tjallingii et al. 2007; Parsons et al. 2013; Weindorf et al. 2014).

The water content of the soil samples varied between 0 % (several sandy soils were completely dried after 2 days) and 136.8 % for saturated soils. The FPXRF concentration attenuations varied between 14.9 and 99.8 % (Table 4). To describe the influence of water content on FPXRF signal, Kido et al. (2006) used inverse functions to fit their data. These functions did not yield satisfactory results for our dataset. The Lambert-Beer law better described the concentration attenuation due to water content in the samples (Table 3). These results are consistent with previous observations (Ge et al. 2005; Tjallingii et al. 2007; Parsons et al. 2013). Even at the higher moisture contents (up to 136.8 %), the analyser was capable of measuring the concentrations of all the studied elements, with the exception of Mn. For this element, no FPXRF signal was detected when the soil moisture was greater than 74.8 % (Table 4).

The regression curves based on the Lambert-Beer law allowed us to determine the attenuation coefficient σ for each element (Table 4). These coefficients are indicators of the water content influence on the FPXRF elemental concentrations. A high σ value for a given element indicates that an increase in water content caused a decrease in the observed FPXRF concentrations.

The FPXRF measurements of Ba, Cr and Sn were the most affected by an increase in water content (Fig. 3a, c, i). Their σ values were the highest: 1.41, 1.28 and 1.03, respectively, and their wet concentrations at the highest moisture content represented less than 25 % of the dry concentrations.

The σ values for Cu, Fe, Mn, Pb, Rb, Sr and Zn were similar, ranging from 0.87 (Sr) to 0.99 (Mn). These elements were less affected by the water content, and the attenuations in the FPXRF concentrations followed a similar trend (Fig. 3). The MAPE values were lower than 15 % for all these elements (Table 4). Calcium was the element for which the water caused the lowest attenuation of FPXRF concentrations, resulting in a σ value of 0.54.

No correlation was observed between the attenuation coefficients (σ) and the atomic numbers of the studied elements.

Table 4 Statistical parameters of FPXRF concentration attenuation (C_{wet}/C_{dry}) and water content regressions

	n	C_{wet}/C_{dry} (%)	Water content (%)	MAPE (%)	σ
Ba	319	99.8–14.9	0.0–136.8	40.6	1.28
Ca	421	99.7–56.1	0.0–136.8	4.9	0.55
Cr	172	98.5–25.0	0.0–136.8	20.4	1.03
Cu	299	96.0–40.6	7.7–136.8	11.3	0.88
Fe	414	99.3–42.1	0.0–136.8	5.4	0.85
Mn	271	99.5–38.1	0.0–74.8	13.6	0.99
Pb	366	99.2–35.8	0.0–136.8	10.7	0.90
Rb	419	98.7–39.4	0.0–136.8	7.8	0.89
Sn	119	97.5–16.7	12.2–136.8	20.6	1.41
Sr	422	98.3–46.4	0.0–136.8	5.0	0.87
Zn	349	99.1–34.3	2.3–136.8	8.8	0.93

σ attenuation coefficient determined according to Eq. (5)

Our results are not in agreement with previous studies (Ge et al. 2005; Kido et al. 2006) that showed that the attenuation of XRF intensities associated with an increase in water content was greater for lighter elements. In the present study, the measurement of a light element, Ca, was the least affected by the soil moisture. The majority of our samples were carbonated, and the mean aqua regia/ICPAES concentration of Ca was high (14.3 %; Table 1). This result could be explained by a concentration effect or could be due to the factory calibration and the built-in algorithm of the analyser.

For each element, the concentration in dry samples was calculated from Eq. (5) using the concentration measured in moist samples and the Lambert-Beer regression curves as follows:

$$C_{\mathrm{dry}} = C_{\mathrm{wet}} \times e^{\sigma\omega} \tag{6}$$

All the studied elements showed very strong correlations between moisture-corrected concentrations and dry sample concentrations ($0.91<R^2<0.99$; Fig. 4 and Table 5). The

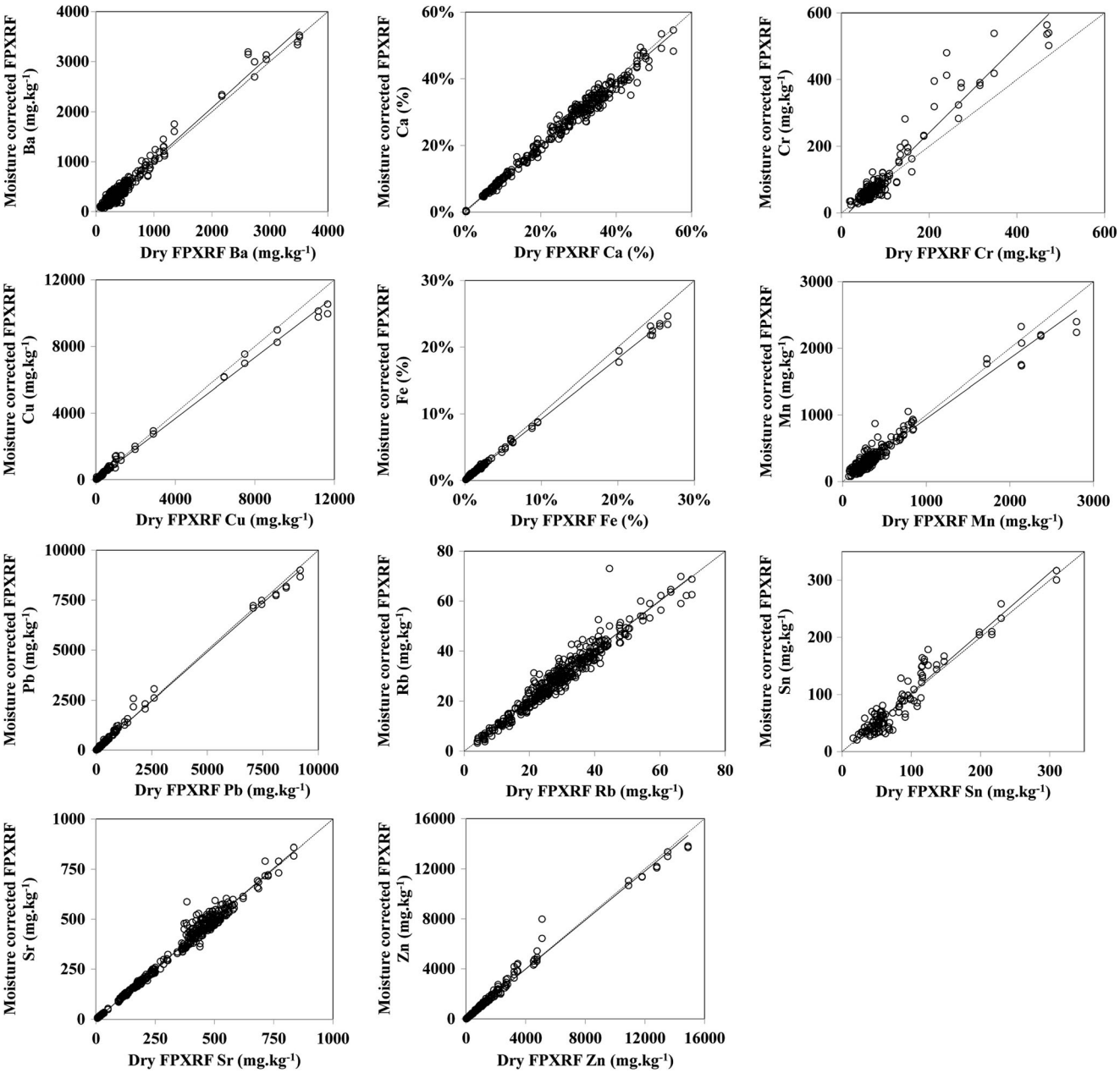

Fig. 4 Regression of moisture-corrected FPXRF concentrations versus dry sample FPXRF concentrations. The regression lines (*straight lines*) and the relation $y=x$ (*dashed lines*) are shown

Table 5 Statistical parameter regressions of moisture-corrected FPXRF vs. dry FPXRF concentrations

	n	R^2	*p* value	Slope	Intercept
Ba	350	0.9722	<0.0001	1.04	−5.5
Ca	430	0.9892	<0.0001	0.97	3722.5
Cr	186	0.9175	<0.0001	1.30	−20.3
Cu	308	0.9959	<0.0001	0.91	25.9
Fe	430	0.9983	<0.0001	0.91	907.9
Mn	308	0.9535	<0.0001	0.90	42.0
Pb	392	0.9961	<0.0001	0.98	15.7
Rb	429	0.9439	<0.0001	1.00	−0.1
Sn	119	0.9166	<0.0001	1.05	−3.0
Sr	430	0.9846	<0.0001	1.00	−1.2
Zn	354	0.9888	<0.0001	0.98	47.6

slopes of the regression equations for Ba, Ca, Cu, Fe, Mn, Pb, Rb, Sn, Sr and Zn are very close to 1 (ranging from 0.90 for Mn to 1.05 for Sn). Only Cr exhibited a slope greater than 1 (1.30), indicating that the moisture correction caused an overestimation of the dry sample concentration. Nonetheless, our results clearly indicate the feasibility of applying moisture corrections to predict the element concentrations of dry soil samples.

4 Conclusions

Ex situ FPXRF analyses of 215 samples showed that FPXRF is a powerful technique to rapidly determine concentrations of Ba, Ca, Cr, Cu, Fe, Mn, Pb, Rb, Sn, Sr and Zn in complex environmental samples, such as soils, with various chemical compositions. The FPXRF results are strongly correlated to those obtained by ICPAES after aqua regia digestion, even though the correlations of certain elements (Fe and Zn) were less satisfactory when concentrations were high ([Fe] >10 %; [Zn] >0.5 %). This difference indicates that the built-in algorithms and factory calibrations of FPXRF analysers may affect the quality of the analyses in certain cases.

For each element, an increase in soil moisture caused a significant decrease in FPXRF concentrations that can be modelled using Lambert-Beer law. The decrease was significant for Ba, Cr and Sn and less marked for Cu, Fe, Mn, Pb, Rb, Sr and Zn. Ca was the element for which the quantification was the least affected by an increase in the water content. Our results suggest that the FPXRF quantifications of major elements with concentrations greater than 10 % are less affected by increases in soil moisture. This issue has never been addressed in previous XRF studies. Further work on the influence of water content on major element quantification by FPXRF should be undertaken to clearly support these findings. This work was beyond the scope of this study because the concentrations of light elements (Al, Si, Na, Mg) were not measured with the FPXRF calibration used (Soil Mode).

Our results obtained from soil samples that span a wide range of physicochemical properties and soil moisture contents showed that the concentrations in soils can be quantitatively predicted using FPXRF and that the effect of water can be satisfactorily corrected. This method represents a serious alternative to chemical methods for the analysis of environmental samples.

Acknowledgments The authors wish to thank the Champagne-Ardenne region for a PhD grant to A. Schneider.

Conflict of interest The authors declare that they have no conflict of interest in this research study and that this one is in agreement with the ethical standards of the COPE guidelines.

References

Arenas L, Ortega M, Garcia-Martinez M, Querol E, Llamas J (2011) Geochemical characterization of the mining district of Linares (Jaen, Spain) by means of XRF and ICP-AES. J Geochem Explor 108:21–26

Argyraki A, Ramsey M, Potts P (1997) Evaluation of portable X-ray fluorescence instrumentation for in situ measurements of lead on contaminated land. Analyst 122:743–749

Bernick MB, Kalnicky D, Prince G, Singhvi R (1995a) Results of field-portable X-ray fluorescence analysis of metal contaminants in soil and sediment. J Hazard Mater 43:101–110

Bernick MB, Getty D, Prince G, Sprenger M (1995b) Statistical evaluation of field-portable X-ray fluorescence soil preparation methods. J Hazard Mater 43:111–116

Binstock DA, Gutknecht W, McWilliams A (2008) Lead in soil by field portable X-ray fluorescence spectrometry, an examination of paired in situ and laboratory ICPAES results. Remediat J 18:55–61

Clark S, Menrath W, Chen M, Roda S, Succop P (1999) Use of a field portable X-ray fluorescence analyzer to determine the concentration of lead and other metals in soil samples. Ann Agric Environ Med 6: 27–32

Frahm E (2013) Validity of "off the shelf" handheld portable XRF for sourcing Near Eastern obsidian chip debris. J Archaeol Sci 40: 1080–1092

Gauss RK, Batora J, Nowaczinski E, Rassmann K, Schukraft G (2013) The Early Bronze Age settlement of Fidvar, Vrable (Slovakia): reconstructing prehistoric settlement patterns using portable XRF. J Archaeol Sci 40:2942–2960

Ge L, Zhang Y, Cheng YS, Zhou SC, Xie TZ, Hou SL (1997) Proposed correction and influence of drilling fluids in X-ray fluorescence logging. X-ray Spectrom 26:303–308

Ge L, Lai W, Lin Y (2005) Influence of and correction for moisture in rocks, soils and sediments on in situ XRF analysis. X-Ray Spectrom 34:28–34

Higueras P, Oyarzun R, Iraizoz J, Lorenzo S, Esbri J, Martinez-Coronado A (2012) Low-cost geochemical surveys for environmental studies in developing countries: testing a field portable XRF instrument under quasi-realistic conditions. J Geochem Explor 113:3–12

Hürkamp K, Raab T, Volkel J (2009) Two and three-dimensional quantification of lead contamination in alluvial soils of a historic mining area using field portable X-ray fluorescence (FPXRF) analysis. Geomorphol 110:28–36

Kalnicky DJ, Singhvi R (2001) Field portable XRF analysis of environmental samples. J Hazard Mater 83:93–122

Kido Y, Koshikawa T, Tada R (2006) Rapid and quantitative major element analysis method for wet fin-grained sediments using an XRF microscanner. Mar Geol 229:209–225

Kilbride C, Poole J, Hutchings T (2006) A comparison of Cu, Pb, As, Cd, Zn, Fe, Ni and Mn determined by acid extraction/ICP-OES and ex situ field portable X-ray fluorescence analyses. Environ Pollut 143: 16–23

Laiho JVP, Perämäki P (2005) Evaluation of portable X-ray fluorescence (PXRF) sample preparation methods. Geol Surv Finl Spec Pap 38: 73–82

Laperche V (2005) Evaluation des performances du spectromètre portable de fluorescence X Niton XL723S (au laboratoire et sur le terrain), BRGM Report 53377-FR, Orléans

Laperche V, Billaud P (2008) The use of portable fluorescence X for the environmental hazard assessment of mining sites: example on the lead mining site at Pont-Péant France, in Post-Mining Symposium, Nancy, France

Mackey EA, Christopher SJ, Lindstrom RM, Long SE, Marlow AF, Murphy KE et al (2010) Certification of three NIST renewal soil standard reference materials for element content: SRM 2709a San Joaquin Soil, SRM 2710a Montana Soil I, and SRM 2711a Montana Soil II. In: NIST Spec. Publ. 260–172, US Department of Commerce and National Institute of Standards and Technology

Papadopoulou D, Zachariadis G, Anthemidis A, Tsirliganis N, Stratis J (2004) Comparison of a portable micro-X-ray fluorescence spectrometry with inductively coupled plasma atomic emission spectrometry for the ancient ceramics analysis. Spectrochem Acta Part B: Atomic Spectrosc 59:1877–1884

Parsons C, Margui Grabulosa E, Pili E, Floor GH, Roman-Ross G, Charlet L (2013) Quantification of trace arsenic in soils by field-portable X-ray fluorescence spectrometry: considerations for sample preparation and measurement conditions. J Hazard Mater 262: 1213–1222

Potts PJ, Webb PC, Williams-Thorpe O, Kilworth R (1995) Analysis of silicate rocks using field-portable X-ray fluorescence instrumentation incorporating a mercury(II) iodide detector: a preliminary assessment of analytical performance. Analyst 120:1273–1278

Radu T, Diamond D (2009) Comparison of soil pollution concentrations determined using AAS and portable XRF techniques. J Hazard Mater 171:1168–1171

Ramsey MH, Potts PJ, Webb PC, Watkins P, Watson JS, Coles BJ (1995) An objective assessment of analytical method precision: comparison of ICP-AES and XRF for the analysis of silicate rocks. Chemical Geol 124:1–19

Scheid N, Becker S, Ducking M, Hampel G, Volker Kratz J, Watzke P, Weis P, Zauner S (2009) Forensic investigation of brick stones using instrumental neutron activation analysis (INAA), laser ablation-inductively coupled plasma-mass spectrometry (LA-ICP-MS) and X-ray fluorescence analysis (XRF). Appl Radiat Isot 67:2128–2132

Somogyi A, Braun M, Posta J (1997) Comparison between X-ray fluorescence and inductively coupled plasma atomic emission spectrometry in the analysis of sediment samples. Spectrochem Acta Part B: Atomic Spectrosc 52:2011–2017

Speakman RJ, Steven Shackley M (2013) Silo science and portable XRF in archaeology: a response to Frahm. J Archeol Sci 40:1435–1443

Tjallingii R, Röhl U, Kölling M, Bickert T (2007) Influence of the water content on X-ray fluorescence core-scanning measurements in soft marine sediments. Geochem Geophys Geosyst Tech Brief 8(2). http://dx.doi.org/10.1029/2006GC001393

Weindorf DC, Bakr N, Zhu Y, Mcwhirt A, Ping CL, Michaelson G, Nelson C, Shook K, Nuss S (2014) Influence of ice on soil elemental characterization *via* portable X-ray fluorescence spectrometry. Pedosphere 24:1–12